ELSEVIER

Journal of Power Sources 111 (2002) 345–349

JOURNAL OF POWER SOURCES

www.elsevier.com/locate/jpowsour

Performance of tin-containing thin-film anodes for rechargeable thin-film batteries

Seung-Joo Lee[a], Heon-Young Lee[b], Sang-Hun Jeong[a], Hong-Koo Baik[a], Sung-Man Lee[b,*]

[a]*Department of Metallurgical Engineering, Yonsei University, Seoul 120-749, South Korea*

[b]*Department of Advanced Material Science and Engineering, Kangwon National University, Chuncheon, Kangwon-do 200-701, South Korea*

Received 9 April 2002; accepted 8 June 2002

Abstract

Thin film, Sn, Cu–Sn and Sn–Zr–(O) anodes for microbatteries are deposited on a copper substrate by radio frequency (rf)-magnetron sputtering at room temperature. Charge–discharge characteristics are compared. It appears that the alloying of Sn with Cu or Zr improves the cycling performance. The best cycling efficiency is obtained when Sn is alloyed with Zr. The effects of alloying elements on the electrochemical properties on the thin film are discussed.

Keywords: Thin film; Anode; Tin-alloying; Microbattery; Cycling performance

1. Introduction

Tin oxide and tin-based composite oxide electrodes have been studied [1,2] as anode materials for lithium rechargeable batteries because of higher capacity compared with graphite. From the viewpoint of high volumetric energy density, it has been suggested [3–5] that tin oxide films are also promising anode materials for rechargeable thin-film microbatteries. With the first charge, the tin oxide decomposes into Li_2O and tin, which leads to a significant amount of irreversible lithium loss. The use of only tin, as an approach to avoid the irreversible loss, has a significant problem in that as lithium is inserted into tin to form Li–Sn alloys, it suffers mechanical instability (cracking) due to large volume difference between the Li–Sn and tin phases. This large volume change limits the cycle life of the electrode.

The research groups of Huggins and coworkers [6–8] have proposed that the performance of an alloy electrode such as Li_xSn can be improved significantly if the active alloying species are finely dispersed with an inactive component in a composite matrix. In this study, therefore, an attempts has been made to apply the same concept to achieve better cycling performance of Sn-based thin-film electrodes. Therefore, Sn, $SnCu_x$ and $SnZr_x$ thin films have been prepared means by for a sputtering method and the electrochemical cycling characteristics of the resulting electrodes have been compared.

2. Experimental

Thin-film electrodes were prepared by depositing Sn, $SnCu_x$ alloy and $SnZr_x$ alloy on copper substrates (12 mm diameter) using a radio frequency (rf) magnetron sputtering system at room temperature. The $SnCu_x$ and $SnZr_x$ thin films were produced by co-sputtering of two pure separate targets. The alloy composition and thickness of the films were controlled by the rf power for each target and the deposition time, respectively. The base pressure in the chamber was 2×10^{-6} Torr and the working pressure was controlled to 5×10^{-3} Torr in the argon atmosphere.

For electrochemical measurements, coin-type test cells were constructed using the film electrodes in 2016 coin cell hardware. The cells used a separator, an electrolyte (1 M $LiPF_6$ dissolved in a 50:50 volume percent (vol.%) mixture of ethylene carbonate (EC) and diethyl carbonate (DE, Cheil Industries Inc., Korea) and a lithium foil for the negative electrode. The cells were assembled and crimped closed in an argon-filled glove box. All cells were tested at 30 a constant current of 50 μA cm^{-2} between 0.0 and 1.2 V.

The surface microstructure of the electrodes was observed by means of scanning electron microscopy (SEM) and X-ray diffraction (XRD) was used to examine the structure of the films. The composition analysis for as deposited films was

---

[*] Corresponding author. Tel.: +82-33-250-6256; fax: +82-33-242-6256.
E-mail address: smlee@kangwon.ac.kr (S.-M. Lee).

0378-7753/02/$ – see front matter © 2002 Elsevier Science B.V. All rights reserved.
PII: S0378-7753(02)00344-0

carried out by Rutherford backscattering spectroscopy (RBS).

3. Results and discussion

The first charge–discharge curves of a tin, thin-film (70 nm thick) electrode are shown in Fig. 1, the charge curve, three potential plateaux appear, as also seen for electroplated tin [8]. The plateaux at 0.69, 0.53 and 0.43 V are associated with the Sn, Li_2Sn_5 and LiSn phases.

The cycling characteristics of tin thin films as a function of film thickness are presented in Fig. 2. The discharge capacity is normalised against the first discharge capacity for each sample. As expected, the cycling performance is little improved by a decrease in film thickness; even for 300 Å thick film capacity fading is still significant after 10 cycles. The cycling behaviour of tin thin films is illustrated by the degradation of the film electrode, as shown by electron micrographs (Fig. 3). In the early stage of cycling (Fig. 3(b)), as a result of large volumetric change with lithium insertion, the formation of large cracks and the delamination of active material from the substrate take place. This leads to a loss of electronic contact between the active materials as well as between the active material and the current collector. Together, these features results in a loss of capacity.

It has been suggested [6–8] that the cycling performance of lithium alloys such as Li_xSn can be improved significantly if intermetallic and/or composite hosts are used instead of pure metals. According to this concept, thin films of tin–metal alloys have been prepared. The voltage profiles of $SnCu_{0.26}$, $SnCu_{0.36}$ and $SnCu_{1.2}$ during the first cycle are shown in Fig. 4. The alloying of tin with copper leads to a reduction in charge–discharge capacity. The voltage profiles of $SnCu_{0.26}$ and $SnCu_{0.36}$ are fairly similar to that of tin shown in Fig. 1. This suggests that these tin–copper alloy films experience a similar mechanism during lithium insertion, that is, the alloying–dealloying of lithium with tin.

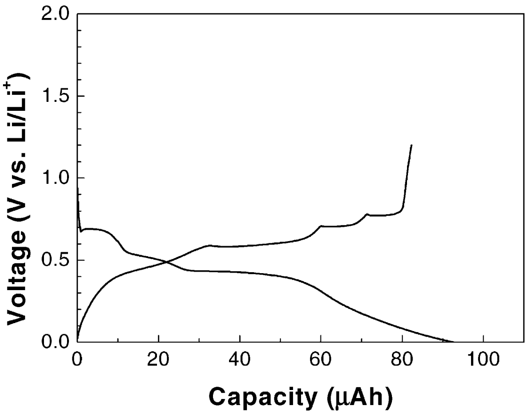

Fig. 1. First charge–discharge curves for tin thin-film electrode.

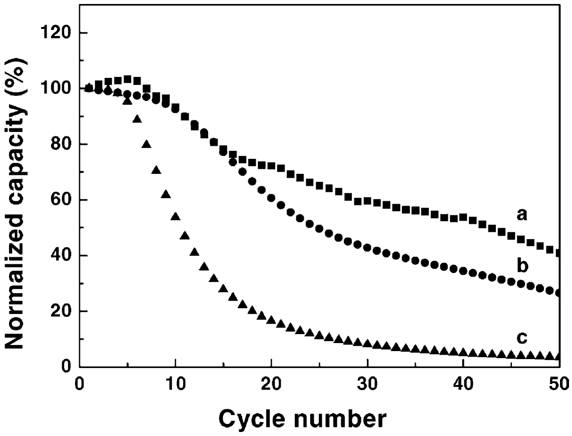

Fig. 2. Normalised capacity vs. cycle number of tin thin-film electrodes of various thickness: (a) 300 Å; (b)700 Å; (c) 1200 Å.

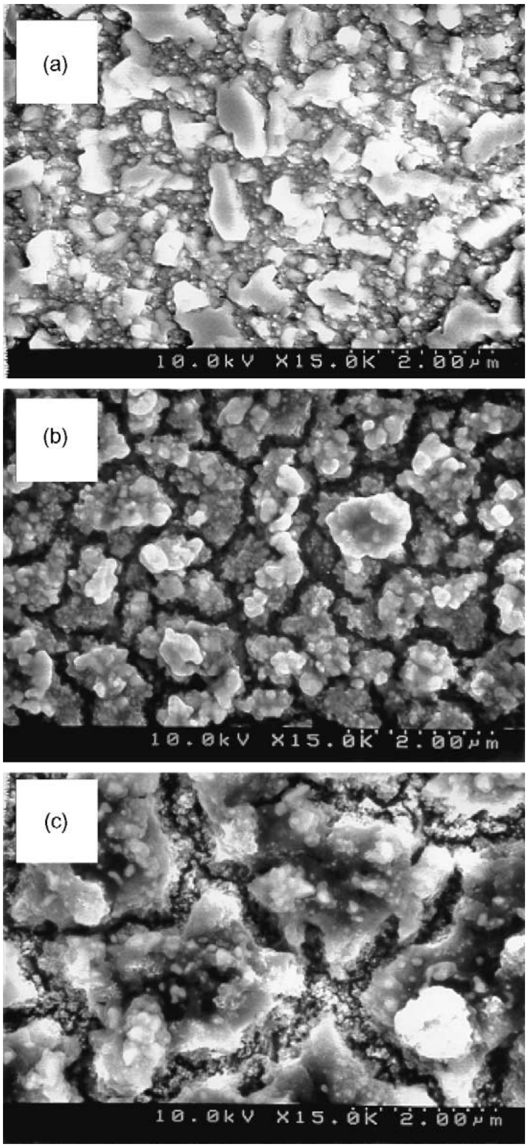

Fig. 3. Electron micrographs (SEM) for thin five film electrode: (a) before cycling; (b) after 6 cycles; (c) after 20 cycles.

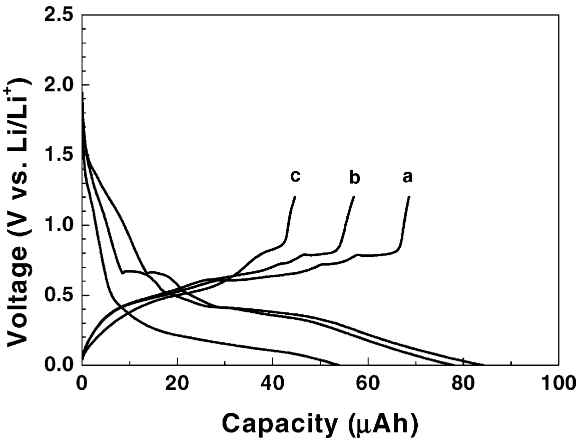

Fig. 4. The first charge–discharge curves for $SnCu_x$ thin-film electrode: (a) $SnCu_{0.26}$; (b) $SnCu_{0.36}$ (c) $SnCu_{1.2}$.

In the case of $SnCu_{1.2}$, it appears that the potential plateaux in the voltage profile are not noticeable because the presence of a substantial amount of spectator element (copper) hinders the formation of the Li–Sn phases.

The discharge capacity versus cycle number of Cu–Sn thin-film electrodes is presented in Fig. 5. Compared with cycle property of a tin thin film (Fig. 2), the Cu–Sn thin films show and enhanced cycle performance, of which the best performance is displayed by $SnCu_{0.36}$. Nevertheless, the capacity fade upon cycling is still significant.

Electron micrographs for the $SnCu_{0.36}$ film electrode before and after cycling are given in Fig. 6. After cycling, a network of cracks is observed on the surface of the film, which is similar to that for a tin thin-film electrode (Fig. 3). This indicates that the inert copper can buffer the volume change of the reactive tin to some extent, but cannot hinder the mobile tin regions from aggregating into larger clusters.

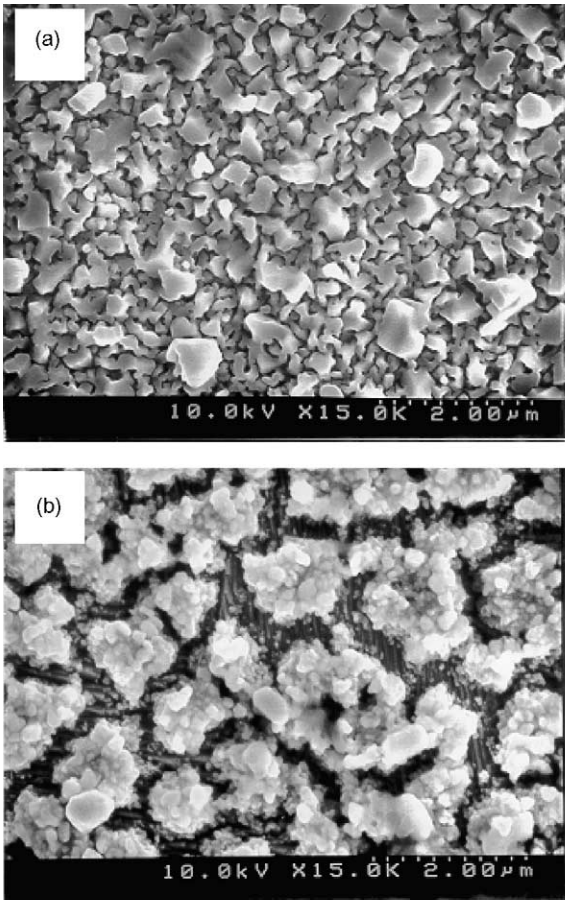

Fig. 6. Electron micrographs of $SnCu_{0.36}$ film electrode: (a) before cycling; (b) after 20 cycles.

The comparison between the values of the enthalpy of formation (ΔH_f) for Li–Sn, Cu–Sn and Zr–Sn systems, as estimated according to the method proposed by the Miedema [9], is presented in Fig. 7. A large negative value for ΔH_f implies a large affinity between atoms in a phase. Therefore, it is expected that Cu–Sn alloys would be broken down to form Li_xSn alloys because of the relatively weak affinity between tin and copper atoms. In fact, the reaction of lithium

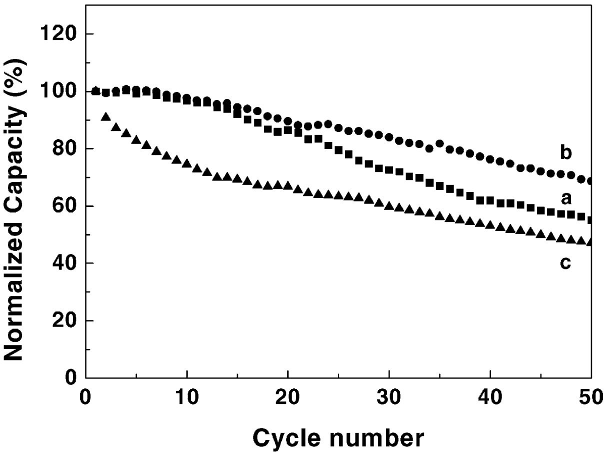

Fig. 5. Normalised capacity vs. cycle number of $SnCu_x$ thin-film electrodes (film thickness: 600 Å): (a) $SnCu_{0.26}$; (b) $SnCu_{0.36}$; (c) $SnCu_{1.2}$.

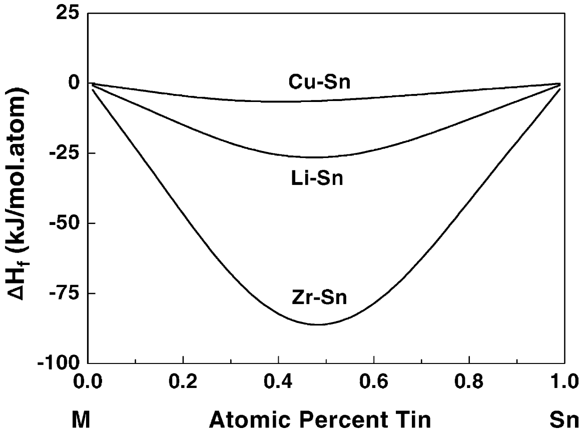

Fig. 7. Calculated heat of formation (ΔH_f) for Li–Sn, Cu–Sn and Zr–Sn binary alloys.

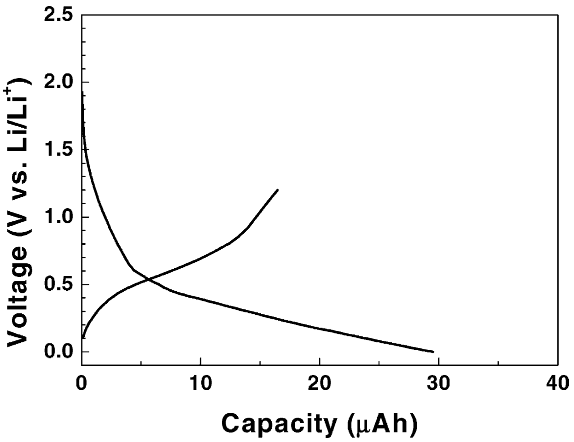

Fig. 8. The first charge–discharge curves for $SnZr_{1.2}O_{0.44}$ thin-film electrode.

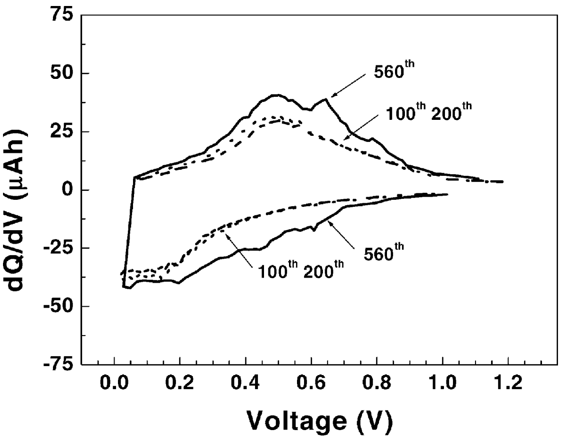

Fig. 10. Differential capacity vs. voltage for 100th, 200th and 560th cycles of $SnZr_{1.2}O_{0.44}$ thin-film electrode.

with Cu_6Sn_5 leads to the formation of $Li_{4.4}Sn$ and copper although, an intermediate Li_2CuSn-type phase is formed [10–12]. On the other hand, the alloying of tin with zirconium may limit lithium alloying with tin form Li_xSn alloys and suppress agglomeration of tin during cycling due to the strong affinity between tin and atoms.

The first charge–discharge curve for the $SnZr_{1.2}O_{0.44}$ thin-film electrode is shown in Fig. 8. The presence of oxygen in the sputtered film is due to traces of oxygen in the sputtering chamber. It is found that most of the oxygen atoms in the film are bounded to zirconium and not tin, as inferred from X-ray photoelectron spectroscopy (XPS) analysis (data not shown here). The voltage profile is very smooth with little evidence of a plateau, which can be seen in the data for tin and Cu–Sn thin films (Figs. 1 and 4). The capacity versus cycle number for the $SnZr_{1.2}O_{0.44}$ thin film is given in Fig. 9. The cycling performance is significantly improved by alloying tin with zirconium, although the effect of oxygen is not clear at present. It is suggested that the enhanced cycleability is because the reaction of tin with lithium is limited by strong bonding between tin and zirconium and/or is blocking the access of lithium to the tin phase. This also cause reduction of the charge–discharge capacity. The capacity increased with cycle number after about 200 cycles, Which becomes more prominent with increase in film thickness, as shown in Fig. 10.

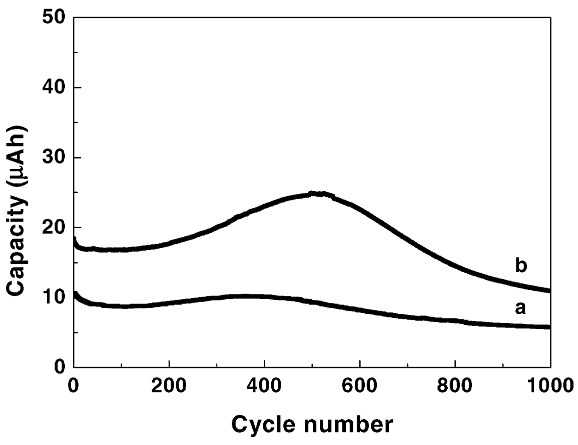

Fig. 9. Capacity vs. cycle number for $SnZr_{1.2}O_{0.44}$ thin-film electrode: (a) 600 Å; (b) 1200 Å.

The differential capacity versus voltage plots for the 100th, 200th and 560th cycles of the film electrode (1200 Å thickness, Fig. 9) are given in Fig. 10. The differential

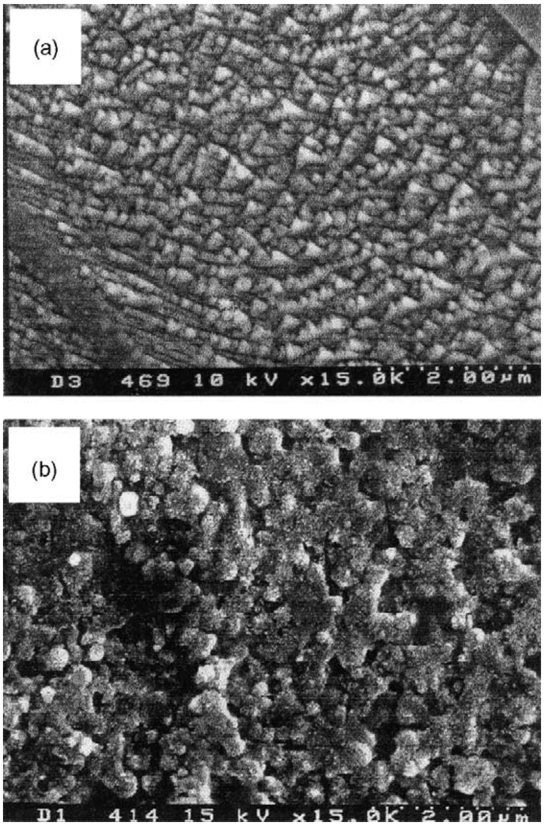

Fig. 11. Electron micrographs of $SnZr_{1.2}O_{0.44}$ film electrode: (a) before cycling (b) after 560 cycles.

capacity shows a broad peak which is stable cycling up to about 200 cycles. On the 560th cycle, however, an additional peak near 0.6 V is presented. This is attributed to the aggregation of tin and Li–Sn alloys into larger grains [13]. In order to confirm that tin and Li–Sn alloys are formed in the film after 560 cycles, ex situ XRD analysis was performed. No clear evidence of small cluster size could be obtained. At this point, it is important to note that aggregation of the tin atoms eventually occurs, even for the $SnZr_{1.2}O_{0.44}$ film. Nevertheless, electron micrographs, Fig. 11, show that the surface of the film electrode has been little modified. Cracks are not observed, even after 560 cycles.

Finally, the present results illustrate that the alloying of tin with an inactive element such as zirconium can enhance significantly the electrode performance. In order to optimise the desired property, however, the composition and microstructure of the thin film need to be further controlled.

4. Conclusions

It has been shown that alloy composite films, prepared through co-sputtering tin and inactive elements (copper, zirconium), improve, the cycling stability of electrodes. Especially, it is suggested that tin films alloyed with zirconium can be strong candidates for thin-film rechargeable battery anodes. These results are consistent with the concept for composite electrodes proposed by the research group of Huggins [6,7] and Winter and Besenhard [8]. It appears that the thermodynamic affinity between tin and inactive elements in a composite electrode plays a crucial role in the enhancement of the dimensional stability of the electrode.

Acknowledgements

This work was supported by the Korean Ministry of Science and Technology through the research programme for "National Research Laboratory."

References

[1] Y. Idota, A. Matsufuji, Y. Maekawa, Miyasaki. Sci. 276 (1997) 1395.
[2] I.A. Courtney, J.R. Dahn, J. Electrochem. Soc. 144 (1997) 2045.
[3] T. Brousse, R. Retoux, U. Herterich, D.M. Schleich, J. Electrochem. Soc. 145 (1998) 1.
[4] S.C. Nam, S. Yoon, W.I. Cho, B.W. Cho, H.S. Chun, K.S. Yun, Electrochem. Commun. 3 (2001) 6.
[5] Y.I. Kim, H.H. Lee, H.S. Moon, K.S. Ji, S.H. Seong, J.-W. Park, J. Power Sources 101 (2001) 253.
[6] R.A. Huggins, Solid State Ionics 113/115 (1998) 57.
[7] R.A. Huggins, in: J.O. Besenhard (Ed.), Handbook of Battery Materials, Part III, VCH, Weinheim, 1999 (Chapter 4).
[8] M. Winter, J.O. Besenhard, Electrochim. Acta 45 (1999) 31.
[9] A.R. Miedema, Philips Tech. Rev. 36 (1976) 217.
[10] K.D. Kepler, J.T. Vaughey, M.M. Thackery, J. Power Sources 81/82 (1999) 383.
[11] K.D. Kepler, J.T. Vaughey, M.M. Thackery, Electrochem, Solid State Lett. 2 (1999) 307.
[12] D. Larcher, L. Beaulieu, D. MacNeil, J. Dahn, J. Electrochem. Soc. 147 (2000) 1658.
[13] I.A. Courtney, W.R. McKinnon, J.R. Dahn, J. Electrochem. Soc. 146 (1999) 59.